



The Fatigue/Fracture Reliability and Maintainability Process and Its Application to Marine Structures

P.H. Wirsching, University of Arizona, Tucson, Arizona
 B. Stahl, Amoco Production Company, Tulsa, Oklahoma
 T.Y. Torng, Southwest Research Institute, San Antonio, Texas
 C.J. Kung, University of Arizona, Tucson, Arizona

ABSTRACT

Structural performance relative to fatigue and fracture of two tendon configurations of a tension leg platform was studied. Reliability methods were employed to account for uncertainties in the design factors. Improvement in reliability over the service life, resulting from a maintenance program of periodic inspection and repair, was quantified. An economic value analysis was performed in order to estimate life-cycle costs associated with the maintenance program of both systems. For the specific structures considered and for an assumed discount rate of 12%, results indicate that, relative to the unmaintained structure, a program of periodic inspection and repair will (a) provide a modest improvement in reliability and (b) result in a slight increase in life-cycle costs.

NOMENCLATURE

a	Crack depth
a_0	Initiation crack depth
a_f	Failure crack depth
a_l	Depth of the largest crack in a tendon
A_C	Length of detected crack
A_0	Cross-sectional area
A_R	Net cross-sectional area (includes crack)
a_{RE}	Threshold repair crack depth
A_I	Fatigue strength coefficient
B	Stress modeling error; a random variable
\tilde{B}	Median of B
B_0	Threshold level for importance sampling
C	Paris coefficient; total expected cost
C_i	Cost of one inspection
C_f	Cost of failure of entire system
C_0	Initial cost
C_{op}	Present value of expected operational costs
C_{ri}	Tendon replacement cost
C_{rp}	Cost of repair of crack
C_F	Present value of expected failure costs
C_I	Present value of expected inspection costs
C_{RP}	Present value of expected repair costs
C_{RL}	Present value of expected replacement costs
C_x	Coefficient of variation of random variable x
COV	Coefficient of variation
DLT	Dynamic load transfer factor (α_3)
F	Peak instantaneous stress prior to fatigue failure
G	Eq. 25
H	Eq. 22
I	Number of inspections
j	Number of tendons that fail
J	Number of joints
K_c	Fracture toughness
m	Fatigue strength exponent
M	Number of tendons
n	Paris exponent

N	Cycles to fatigue failure
N_I	Cycles to fatigue crack initiation
N_D	Crack propagation cycles to failure
N_s	Cycles in service life
N_T	Total cycles to fatigue failure
P_d	Probability of detecting crack
P_f	Probability of failure
P_{PL}	Platform loss probability
P_{RL}	Probability of replacement
$P(D)$	Probability of detection curve
POD	Probability of detection
$Q(t)$	Force on system
R_B	Ultimate strength, brittle fracture
R_D	Ultimate strength, ductile fracture
S	Stress range
S_e	Equivalent stress range
S'_e	Equivalent stress range, best estimate
S_E	Extreme stress
S'_E	Extreme stress, best estimate
S_f	Random variable denoting stress range at fatigue
S_F	Impulsive stress, fatigue failure
S_I	Impulsive stress, fracture failure
S_0	Stress range having return period of N_T cycles
T	Time to failure
T_s	Service life
Y	Geometry factor
α_1	System redistribution factor
α_2	Load redistribution factor
α_3	Dynamic load transfer factor
$\Gamma(\cdot)$	Gamma function
γ	Annual discount rate
ξ	Weibull shape parameter
Φ	Standard normal distribution function
σ_{lnA}	Standard deviation of \ln of A_C

INTRODUCTION

Because of large uncertainties in fatigue and fracture design factors, reliability methods are useful for the engineering decision-making process relative to large marine structures subjected to dynamic loads. For structures which "age" or deteriorate with time, the lifetime integrity, as measured by reliability, will improve with a maintenance program of periodic inspection and repair; but, a maintenance program can be expensive. Ultimately, the goal of analysis should be to prescribe a design along with a maintenance program to minimize the total expected life-cycle cost.

This particular study deals with the fatigue/fracture reliability and maintainability (FRM) process of the tendon system of a tension leg platform (TLP). The TLP is a novel design of an oil platform for use offshore. A sketch of a TLP is shown in Figure 1. The design uses a floating hull, which is moored to the seabed

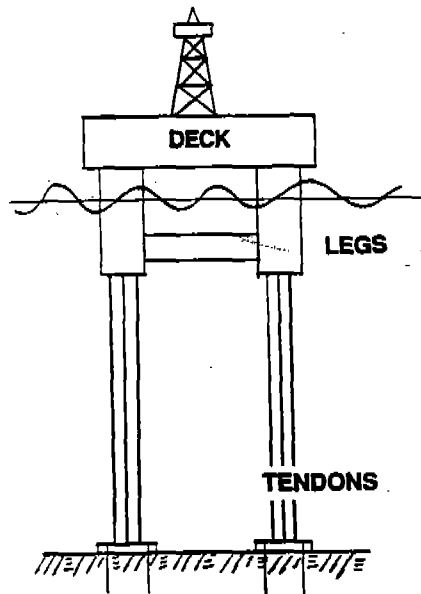


Figure 1. Tension leg platform (TLP).

by vertical mooring lines or tendons. Excess buoyancy of the hull maintains a tensile force on the tendons, providing the stability required for operation of the platform. Compared to the fixed-bottom-founded structure, the primary advantages of this type of platform are its economic potential for use in deeper water and at marginal fields, as the hull can be towed to a new site and re-used. Typically, a TLP will have four legs. Designs having two, three, or four tendons per leg are under consideration.

Several simplifying assumptions are made in the analysis. Not included were considerations of (1) stress corrosion, (2) gross yielding in a tendon, (3) notch effects in fatigue, (4) stress modeling error applied separately to each tendon or joint, (5) quasi-static failure by the n th largest stress, (6) continuous monitoring for cracks, (7) errors in crack measurement, (8) false positives, (9) finite time to make repairs, and (10) possible poor quality of the repaired tendons. Also, it was assumed that the deck elevation was set sufficiently high so that the probability of failure due to wave impact of the deck is relatively small.

THE STRUCTURAL MODEL

The structure considered is a TLP tendon system modeled as a parallel/series system (Figure 2). The tendons are assumed to be dominated by tensile loading, and the two failure modes are fatigue and fracture. Discrete failure sites for fatigue and brittle fracture are shown as notches. These correspond to joints, i.e., stress concentrations, in each tendon.

The external load, $Q(t)$, is a random process. Under $Q(t)$, failure in a tendon can occur due to fatigue failure at any joint, a brittle or ductile fracture from an extreme load, or impulsive loading resulting from failure of another tendon. It will be assumed that system failure occurs if all M tendons of a leg fail.

Two TLP systems will be analyzed: a 4-tendon leg and a 2-tendon leg. The water depth is 2500 feet, and there will be 4 legs and 80 joints per tendon. A summary of all the data used in the analysis is provided in Table 1.

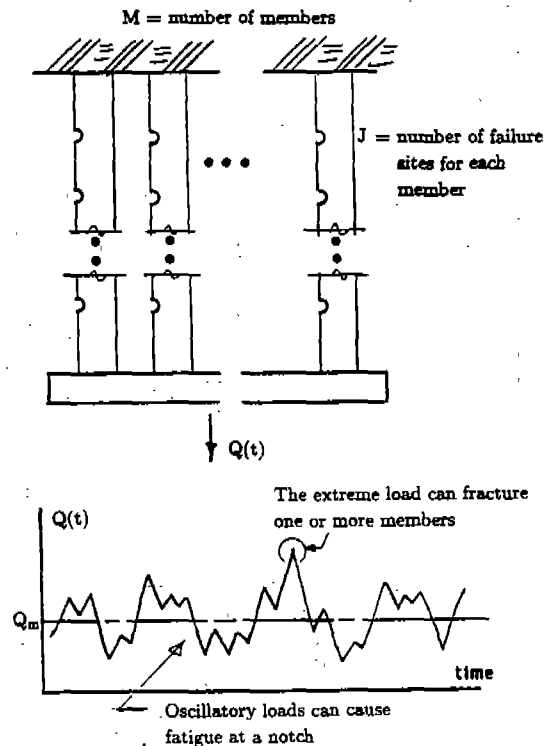


Figure 2. Loads applied to a parallel/series structural model of the tendons in one leg.

LOADING IN TENDONS

It is assumed that (1) each tendon carries an equal load; (2) the axial stress will be constant throughout each tendon; and (3) after failure of one tendon, the stresses will be equal in and uniform throughout the remaining tendons. For design and analysis purposes, the following must be defined: (1) fatigue stresses, (2) extreme stress (the maximum expected stress in the service life), and (3) separation stress (the stress in remaining tendons after one tendon has failed).

Fatigue Stress Distribution

For fatigue analysis of marine structures, it is commonly assumed that the long-term distribution of stress ranges is Weibull [1]. The parameters that define the stress environment for the systems considered are given as

$$N_T = 10^7 \text{ cycles}$$

$$S_0 = \begin{cases} 17.3 \text{ ksi (4 tendons)} \\ 12.2 \text{ ksi (2 tendons)} \end{cases}$$

$$\xi = 1.5$$

where N_T is the total number of cycles in the service life, S_0 is the stress range for which the probability of exceedance is $1/N_T$ (or the event of a stress range exceeding S_0 has a return period of N_T cycles), and ξ is the Weibull "shape parameter." A specific fatigue model, $NS^m = A$, is assumed. Then, because S is Weibull, the equivalent constant-amplitude (Miner's) stress is

Table 1. Summary of the data.

	4 Tendons	2 Tendons
Tendon length (ft)	2400	2400
Length/element (ft)	30	30
Number of joints for each tendon	80	80
Dimensions of tendon		
Diameter (in.)	24.0	42.0
Wall thickness (in.)	1.0	1.625
Area (in ²)	75.4	214
Cross-sectional area of one leg (in ²)	301	428
Service life		
T _s (yrs)	20	20
Cycles of fatigue stress	10 ⁷	10 ⁷
Extreme load, S _E		
Median, S̄ _E (ksi)	36.0	25.3
COV, C _s	0.20	0.20
Fatigue load		
S ₀ (ksi)	17.3	12.2
ξ	1.5	1.5
N _T	10 ⁷	10 ⁷
Miner's stress, S _e (ksi)	3.42	2.42
Separation shock, S̄ (first tendon fatigue)		
Median, S̄ (ksi)	44.8	47.3
COV, C _s	0.158	0.158
Probability of detection curve, P(a) _i lognormal		
Median (in.)	0.222	0.222
COV	0.514	0.514
Modeling error, B (same for fatigue and fracture)		
Median, B̄	1.00	1.00
COV, C _B	0.20	0.20
Ultimate strength, R		
Median, R̄ (ksi)	80	75
COV, C _R	0.08	0.08
Fracture toughness, K _C (ksi√in.)		
Median, K̄	200	200
COV, C _K	0.15	0.15
Crack initiation, NS ^m = A		
A (ksi units)	1.15E9	8.05E8
C _A	0.63	0.63
m	3.0	3.0
Initiation crack size (in.)	0.02	0.02
Crack propagation, Paris law		
C (ksi units)	5.24E-10	5.24E-10
C _C	0.63	0.63
m	3.0	3.0
ΔK _{th} (ksi√in.)	0	0
Geometry factor, Y	1.12	1.12
Failure crack length (in.)	20	20
Minimum crack depth for repair (in.)	0.20	0.20

$$S'_e = S_0 [\ln N_T]^{-1/\xi} \Gamma^{1/m} \left[\frac{m}{\xi} + 1 \right], \quad (1)$$

where $\Gamma(\cdot)$ is the gamma function and the prime indicates the stress as predicted by the "best" available analytical method. For the case of $m = 3$ used in this analysis (as described later) and the above values, Miner's stress is

$$S'_e = \begin{cases} 3.42 \text{ ksi (4 tendons)} \\ 2.42 \text{ ksi (2 tendons)} \end{cases} \quad (2)$$

Extreme Stress

Using the best predictive analytical method, the extreme stress, S'_E , in each tendon is equal to

$$S'_E = \begin{cases} 36.0 \text{ ksi (4 tendons)} \\ 25.3 \text{ ksi (2 tendons)} \end{cases} \quad (3)$$

This is the 20-year return-period stress. A breakdown of the components of S'_E is provided in Table 2.

Table 2. Components of extreme stress (in ksi).

	No. of Tendons	
	4	2
Pretension	21.0	14.8
Design wave stress amplitude, S ₀ /2	8.7	6.1
Wind, current, and tide	6.3	4.4
Total, S' _E	36.0	25.3

Stress Modeling Error

Stress modeling error is associated with uncertainties in assumptions made in the stress analysis and is

quantified by the random variable B, defined as

$$B = \frac{\text{actual stress in component}}{\text{predicted stress in component}} \quad (4)$$

having a median $\tilde{B} = 1.0$ and coefficient of variation $C_B = 0.20$. B is assumed to have a lognormal distribution. These figures are based on studies of stress modeling error [1]. The random variable B is applied to both the extreme load and to fatigue stress.

The equivalent constant-amplitude fatigue stress is

$$S_e = B S'_e \quad (5)$$

and the extreme stress is

$$S_E = B S'_E \quad (6)$$

Clearly, both S_e and S_E are random variables by virtue of their functional relationship to B.

Impulsive Separation Stress

Upon failure of one tendon, there will be a redistribution of loads throughout the entire tendon system. The full load carried by one leg before tendon failure is not shed to the remaining tendons of that leg after failure because, due to a shift in buoyancy, there is a transfer of load to all the other tendons of the other legs. Adding to the complexity of the problem is the fact that failure is likely to occur under extreme environmental conditions, at which time it is difficult to predict the dynamic response of the system and the corresponding loads in the surviving tendons.

The model for impulsive separation stress used herein is elementary and must be considered as a first approximation only. The impulsive separation stress is treated two ways, depending upon the mode of the first tendon failure.

First Tendon Failure is Fracture. Brittle or ductile fracture can occur in one or more tendons under an extreme load. It is assumed that tendon failure is instantaneous, so the load is transferred to the remaining intact tendons of the TLP system. The load is modified by three factors that relate to the mechanics of the TLP system. Following failure, the peak impulsive stress in the intact tendons can be written as

$$S_1 = (\alpha_1 \cdot \alpha_2 \cdot \alpha_3) S_E \quad (7)$$

where α_1 = system redistribution factor (SRF)—accounts for load sharing throughout the entire TLP tendon system following the failure of one or more tendons; α_2 = load redistribution factor (LDF)—accounts for load transfer in a single leg; and α_3 = dynamic load transfer (DLT) factor—accounts, in a single leg, for any impulsive dynamic response in addition to the static response defined by α_2 . Values of α_1 are summarized in Table 3. They are derived using a static analysis of the entire TLP having a missing tendon(s) in one leg. Assuming that there is equal load sharing,

$$\alpha_2 = \frac{M}{M-j} \quad (8)$$

where M is the number of tendons per leg and j is the number of tendons that fail. In general, $\alpha_3 \geq 1.0$, with equality when there is heavy damping in the system. The general expression for α_3 with no damping is

$$\alpha_3 = 2 - \frac{M-j}{M} \quad (9)$$

Table 3. System redistribution factor α_1 .

Number of Tendon Failures	4 Tendons	2 Tendons
1	0.910	0.790
2	0.642	—
3	0.338	—

First Tendon Failure is Fatigue. Because fatigue is modeled as an equivalent constant-amplitude process, failure in a tendon is assumed to occur when the largest crack in the tendon becomes too large. This failure can occur in any sea state. It is assumed that, in the instant prior to failure, the stress F will be the peak (tensile) instantaneous stress in the sea state. The goal will be to estimate the statistical distribution of the random variable F. Then, the peak impulsive stress in the remaining intact tendons will be

$$S_F = (\alpha_1 \cdot \alpha_2 \cdot \alpha_3) F \quad (10)$$

In order to construct the distribution of F, the following assumptions are made: (1) The fatigue failure stress F will be bounded from below by the static pretension S_p . (2) The extreme stress S_E defines the right tail. (3) The distribution of F will follow the distribution of stress ranges at fatigue failure, a random variable denoted as S_f . (4) The distribution of S_f is equal to that of S, the long-term distribution of stress ranges, weighted by the crack growth rate, S^m , to account for increased vulnerability in higher sea states. The corresponding pdf for F, denoted as f_F , can be derived in a straightforward manner by a change of coordinates:

$$F = \frac{S_f}{S_0} (S_E - S_p) + S_p \quad (11)$$

As a practical matter, the Type I extreme value distribution is fitted to the hybrid distribution as described above. The fit is made by requiring that (1) the mode of each be the same and that (2) the right tail area of each, beyond S_0 , be the same.

FATIGUE STRENGTH

The fatigue model will consider both crack initiation and crack propagation. Total fatigue life (cycles to failure) is

$$N_T = N_I + N_p \quad (12)$$

where N_I is the number of cycles to initiate a crack of specified length a_0 , and N_p is the number of cycles to grow the crack from a_0 to fracture. Fatigue failure is defined as the event of first passage of the crack length a of level a_f , the fracture crack length.

Initiation life is described by the characteristic S-N curve

$$N_I S^m = A_1 \quad (13)$$

where m and A_1 are the fatigue strength exponent and coefficient, respectively. For probabilistic analyses, m is assumed to be a constant and A_1 is a lognormally distributed random variable reflecting the inherent variability of fatigue strength. The stress range S is of constant amplitude (or its equivalent). Equation (13) implies high cycle fatigue with no stress endurance limit.

Propagation life is obtained from an integration of the Paris law, assumed to describe crack growth,

$$N_p = \frac{1}{CS^n \pi a_0^{n/2}} \int_{a_0}^{a_f} \frac{da}{Y^n(a) a^{n/2}}, \quad (14)$$

where n and C are the Paris exponent and coefficient, respectively; Y is the geometry factor; a_0 is the initiation crack depth; and a_f is the failure crack length. The threshold stress intensity level is assumed to be zero. C is modeled as a lognormal variate reflecting the uncertainty in the crack growth rate, and n is assumed to be constant. Fatigue strength properties (A_1 , m , C , n) used in the study were obtained from data presented by Almar-Ness [2] and Mohaupt et al. [3] and are summarized in Table 1.

FRACTURE STRENGTH

It is assumed that a tendon can experience a ductile or brittle fracture under the extreme stress, S_g , or under the impulsive shock stresses, S_1 or S_F . The onset of failure of a tendon is defined as

$$\text{Stress in Tendon} > \min(R_D, R_B)$$

where

$$R_D = R_u \cdot \frac{A_R}{A_0} \quad (\text{ductile fracture}) \quad (15)$$

$$R_B = \frac{K_c}{Y(a_1)\sqrt{\pi a_1}} \quad (\text{brittle fracture}) \quad (16)$$

and where R_u and K_c are the ultimate strength and fracture toughness, respectively, and are both considered to be random variables. A_R is the net cross-sectional area (original area minus cracked area) and A_0 is the original cross-sectional area; a_1 is the depth of the largest crack in a tendon. Statistics on R_u , K_c , and Y are presented in Table 1.

PROBABILITY OF DETECTION

At inspection, the chance of finding a crack obviously increases as the crack size increases. The probability of detection (POD) curve is assumed to have a lognormal form with a median, $\tilde{A}_C = 0.222$ in., and COV, $C_{AC} = 0.514$. The lognormal form of the POD curve is not only easy to use but is similar in form to other POD curves which have been published. Thus, the probability of detection for crack length a is

$$P(D) = \Phi(z), \quad (17)$$

where Φ is the standard normal distribution function,

$$z = \frac{\ln(a/\tilde{A}_C)}{\sigma_{\ln A}} \quad \sigma_{\ln A} = \sqrt{\ln(1 + C_{AC}^2)}$$

It is assumed that measurement of the size of the detected crack is accurate.

REPAIR DECISION

Generally, it is not considered economically feasible to repair small cracks that are judged to be non-dangerous. For this analysis, the minimum crack depth for repair, a_{RE} , is assumed to be 0.20 in. Assuming a

crack aspect ratio of $a/2c = 0.10$, the surface crack length is 2.0 in.

Repair will be done on all detected cracks $a > a_{RE}$. This decision rule is considered to be safe because the estimated median life remaining is 2.7×10^7 cycles (using crack growth data presented in the following), whereas the service life is 10^7 cycles. It is assumed that the repairs are performed "instantaneously" and that the repaired tendon is like new.

ANALYSIS OF THE FRM PROCESS

Clearly, the fatigue/fracture reliability and maintainability (FRM) process is extremely complicated. The principal goal of analysis is to derive the distribution of time to system failure, T . Secondary goals are to construct the hazard function, conditional probability functions given survival at any time, repair rates for cracked and failed tendons, etc.

Monte Carlo simulation looks attractive as a solution strategy because of the complexity of the process. Direct Monte Carlo simulation of the tendon system is not a practical possibility because of (1) the physical size of the system, i.e., 320 fatigue elements in the 4-tendon system; (2) the large number of random variables, i.e., about 650 in the 4-tendon system; and (3) the small probability of a failure event. Thus, an "efficient" method based on limited sampling must be employed.

A simple importance sampling scheme was employed as follows: While there are a large number of random variables in the process, B (stress modeling error) plays a dominant role. A very simple importance sampling scheme was found to be effective. The sampling distribution is the density function of B , f_B , for $B_0 \leq B < \infty$, where B_0 is a value below which no failures are expected. The value B_0 was found by a trial-and-error process. This method has proved to be relatively efficient. Nevertheless, there are other random variables in the problem, and development of a more powerful scheme for importance sampling would be appropriate.

RESULTS OF ANALYSIS

Results of the analysis by simulation of the performance of one leg is summarized in Figure 3. The probability of failure of one leg is given as

$$p_1 = \Phi(-\text{BETA}) \quad (18)$$

where Φ is the standard normal distribution function and BETA is the safety index. Relative steel weights of the two systems are given to demonstrate, in part, why the 2-tendon system has a significantly higher reliability. Results are presented in terms of the dynamic response following fracture of a tendon. The DLT (α_3) values in Figure 3 bound the response: DLT = 1.0, no dynamic impulse response; and DLT = 1.5 or 1.25, no damping, as per Eq. (9).

It was assumed that loss of the platform would result from the failure of any leg. Platform loss probability was approximated by

$$P_{PL} = 4 p_1 \quad (19)$$

Using this approximate form, the reliability and maintenance performance of the entire platform was estimated and is summarized in Table 4. The 90% confidence intervals for probability of failure estimates

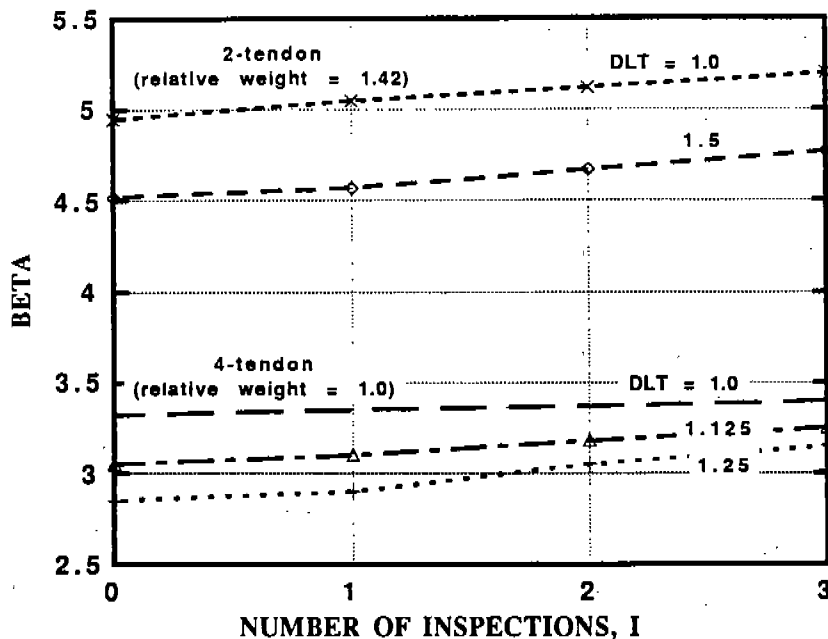


Figure 3. Safety index of one leg during the service life as predicted prior to service.

Table 4. Performance summary of entire structure with four legs (DLT = 1.0).

	4 Tendons		2 Tendons	
	Probability ^a in 10 ⁻³		Probability ^b in 10 ⁻⁶	
	I = 0	I = 3	I = 0	I = 3
Failure (P _{Pl})	1.80	1.38	1.20	0.43
Fatigue-initiated failure	0	0	0.16	0.08
Failure under extreme load	1.80	1.38	1.04	0.35
Repair of tendon broken by fatigue	97.20	39.10	26.40	10.80
Repair of tendon broken by extreme load	3.30	1.34	0	0
Crack discovered and repaired	0	45.20	0	16.40

^aExpected number of occurrences in a thousand structures.

^bExpected number of occurrences in a million structures.

are about ±7% for the 4-tendon system and ±10% for the 2-tendon system.

TOTAL EXPECTED LIFE-CYCLE COSTS

An economic value analysis was performed on both tendon systems to estimate total life-cycle costs. The present value of the total expected cost can be written as

$$C = C_0 + C_{op} \quad (20)$$

where C_0 = the initial cost and C_{op} = the present value of the expected operational costs,

$$C_{op} = C_F + C_I + C_{RP} + C_{RL} \quad (21)$$

where C_F , C_I , C_{RP} , and C_{RL} are the present values of the expected failure, inspection, repair, and replacement costs, respectively.

Inspection. Scheduled inspections occur at discrete times, t_i . Assuming continuous discounting, the present value of future payments for I inspections is

$$C_I = C_i H(\gamma) \quad (22)$$

where

$$H(\gamma) = \sum_{i=1}^I e^{-\gamma t_i} \quad (23)$$

C_i = the cost of one inspection, and γ = the annual discount rate.

Repair of Crack Discovered at Scheduled Inspection. Let C_{RP} be the cost of repair of a crack detected at a scheduled inspection, t_i . The expected present value of these future costs is

$$C_{RP} = \frac{C_{RP} P_d H(\gamma)}{I} \quad (24)$$

where P_d is the probability that a crack will be detected during the service life. This form assumes that there will be an equal number of repairs at each inspection.

Replacement of Broken Tendons. Tendons can experience fatigue or fracture at any time during the service life, T_s . Assuming that the rate of occurrence of replacements is a linearly increasing function, the present value of the expected replacement cost is

$$C_{RL} = P_{RL} C_{rt} G(\gamma, T_s), \quad (25)$$

where

$$G(\gamma, T_s) = \frac{2[1 - e^{-\gamma T_s}(\gamma T_s + 1)]}{(\gamma T_s)^2}, \quad (26)$$

C_{rt} is the replacement cost at any time t , and P_{RL} is the estimated probability of replacement. T_s is the service life, which is 20 years in this study.

Failure. Loss of the platform is assumed to occur when there is tendon failure in one leg. The present value of the expected failure cost is

$$C_F = P_f C_f G(\gamma, T_s), \quad (27)$$

where P_f = the probability of failure of the entire tendon system and C_f = the cost of failure of the entire system.

Expected life-cycle costs are estimated for the 2- and 4-tendon systems. These estimates are summarized in Table 5. The results in Table 5 indicate that while the initial cost of the 2-tendon system is higher (because it has more steel), failure and repair costs are lower, reflecting relatively low stresses. For both systems, the investment in inspection is not exceeded by the reduction

in failure and repair costs, i.e., inspection is not cost effective for the two models considered.

SUMMARY

As suggested by the results presented in Figure 3, a maintenance program for the specific systems considered herein is only moderately effective. This may be explained by the fact that crack initiation life is relatively "long" and crack growth rates are relatively high. As shown in Table 4, with three inspections, only about half the cracks are found and repaired before tendon fatigue failure occurs. Moreover, there seems to be a relatively high incidence of tendon fatigue failures; yet, few of these lead to loss of the platform.

ACKNOWLEDGMENTS

The writers acknowledge J. F. Geyer, Amoco Production Company, and D. I. Karsan, Conoco Inc., for their insights and expertise in developing basic model parameters for the example TLP tendon systems.

REFERENCES

1. P. H. Wirsching and Y. N. Chen, "Considerations of Probability Based Fatigue Design for Marine Structures," *Marine Structures* 1, 1988, 23-45.
2. A. Almar-Ness (Ed.), *Fatigue Handbook: Offshore Steel Structures*, Tapir, 1985.
3. V. H. Mohaupt, D. J. Burns, J. G. Kalbfleisch, D. Vosikovskiy, and R. Bell, "Fatigue Crack Development, Thickness, and Corrosion Effects in Welded Plate to Plate Joints," in *Steel in Marine Structures*, Elsevier, 1987.

Table 5. Summary of cost analysis (20-year service life).

● Present Costs (millions of dollars)				
	4 Tendons		2 Tendons	
Initial cost of tendon system	35		48	
Failure cost of platform	1000		1000	
Repair cost of cracked tendon	3.5		5.0	
Replacement cost of broken tendon	7.0		10.0	
Cost of inspection	0.80		0.50	
● Expected life-cycle costs of TLP tendon systems (includes all four legs) Discount rate = 12%; Dynamic load transfer (DLT) factor $\alpha_3 = 1.0$				
	4 Tendons		2 Tendons	
	I = 0	I = 3	I = 0	I = 3
Operational costs				
Failure	0.432	0.340	0.0003	0.0001
Inspection	0	0.820	0	0.5100
Repair	0	0.054	0	--
Replacement	0.163	0.069	0.0001	--
Total	0.595	1.283	0.0004	0.5101
Initial cost	35.0	35.0	48.0	48.0
Total cost	35.60	36.28	48.00	48.51

DISCUSSION

Walter Maclean

You say that, as your end conclusion, you can't use this as a model to suggest that maintenance is cost effective, but on the other hand you made note of the fact that the four-tendon system was significantly redundant. Wouldn't that also suggest that the redundancy is making up for the lack of cost effectiveness in maintenance? The more redundancy you have, the less maintenance you can do and still survive.

Paul Wirsching

Yes, absolutely - when we think in terms of insuring reliability; the two important factors are redundancy and inspection and of course the two are intimately related.

Jack Mercier

There are two tension leg platforms in service and Conoco operates both of them so I think I should give a little status report on the inspection programs for the tension legs of these two systems. There are two different kinds of tension legs, the first one for the up field in the North Sea uses threaded connectors. We have spent something in the order of 15 million dollars to develop a workable inspection system that can inspect these tension legs *in-situ*. We have also the experience of removing and subsequently replacing the entire tension leg with the cost of about a quarter of a million dollars per tension leg. I think perhaps we had a better solution by removing and replac-

ing rather than developing the *in-situ* tool. The other tension leg platform at Joliet Field in the Gulf of Mexico has all-welded, one piece tendons and an inspection device has been developed for those as well, but it is still in the process of being proven in the course of the first year's inspection program. The cable that runs the ultrasonic device's internal inspection inside the tension leg parted and it has had to be remade in a more robust form so that the full inspection can be done.

I'm a little surprised about the lessons of inspection not being particularly relevant from your analysis, Paul. If that were the case, it would bolster the argument in favor of building the tension legs so robust that inspection is not necessary and I think that's an ideal solution if it can be done. However, it does have the problem that the process of installing a tension leg may well change its characteristics from the time when it was built. Some kind of confirmation of adequacy of the tension leg after it's installed would be needed.

Paul Wirsching

When we did this analysis and constructed a probability of detection curve we really had no idea how inspection would be carried out. Furthermore I'd like to mention a number of people have reviewed this work and there is a tendency, I think, to try to draw too many conclusions from this. Again I want to point out that we make an awful lot of assumptions here and some of them would significantly influence the results.